



HAL
open science

Automated method for designing extractive dividing wall columns used to separate minimum azeotropic mixtures with a heavy entrainer

Fatima-Zohra Seihoub, Vincent Gerbaud, Hassiba Benyounes

► To cite this version:

Fatima-Zohra Seihoub, Vincent Gerbaud, Hassiba Benyounes. Automated method for designing extractive dividing wall columns used to separate minimum azeotropic mixtures with a heavy entrainer. *Chemical Engineering Research and Design*, 2024, 207, pp.361-372. <10.1016/j.cherd.2024.05.041>. <hal-04690097>

HAL Id: hal-04690097

<https://ut3-toulouseinp.hal.science/hal-04690097v1>

Submitted on 6 Sep 2024

HAL is a multi-disciplinary open access archive for the deposit and dissemination of scientific research documents, whether they are published or not. The documents may come from teaching and research institutions in France or abroad, or from public or private research centers.

L'archive ouverte pluridisciplinaire **HAL**, est destinée au dépôt et à la diffusion de documents scientifiques de niveau recherche, publiés ou non, émanant des établissements d'enseignement et de recherche français ou étrangers, des laboratoires publics ou privés.



HAL Authorization

Automated method for designing an extractive dividing wall column: 1. Minimum azeotropic Mixtures with a Heavy Entrainer, class (1.0-1a)-m1

Fatima-Zohra Seihoub^{a,*}, Vincent Gerbaud^b, Hassiba Benyounes^{a,c}

^a Université des Sciences et de la Technologie – Mohamed Boudiaf, Oran, Algérie

^b Laboratoire de Génie Chimique, Université de Toulouse, CNRS, INP, UPS, Toulouse, France

^c UST. Oran, Laboratoire de chimie physique de matériaux, catalyse et environnement, Oran, Algérie

Highlights

- The proposed E-DWC design method was constructed with the help of the composition profile properties in the *ISS* mode.
- The separation feasibility delimitation is solely a function of the phase equilibrium constant (k_i) along the sides of the composition simplex.
- Because of its generalized formula, the use of the difference point equation to determine trajectories in different sections of the E-DWC is very advantageous for the automation of the method.
- The method presented in this paper is the first to determine extractive trajectories using the difference point equation (DPE).

Abstract

Despite that the extractive divided wall column (E-DWC), which is one of the best examples of process intensification, has already found an industrial application, its design remains a new area of research. None of the few studies that have been published in the literature present a method for designing an E-DWC. Therefore, the first and fully automated design method, for the separation of minimum boiling azeotropic mixtures with a heavy entrainer (class (1.0-1a)-m1) using an extractive dividing wall column, is developed in this work. The developed method is based on the values of the phase equilibrium constant along the sides of composition simplex, with the help of the composition profile properties in the infinitely sharp splits mode and difference point equations. The efficiency of this new design method was tested on the separation of two ternary azeotropic mixtures that belong to class 1.0-1a-m1. The results show that the column trajectories, along the E-DWC, obtained by the

rigorous simulation are in very good agreement with those calculated by the new design method. These results prove the reliability and accuracy of the new method.

1. Introduction

Separation of azeotropic mixtures has been for many years a challenging field of chemical engineering. Among common techniques, like azeotropic distillation or pressure swing distillation, extractive distillation is a widely used process for the separation of homogeneous azeotropic mixtures because of its low energy consumption and high product purity (Sucksmith, 1982; Lei et al., 2003; Aniya et al., 2018; Gerbaud et al., 2019). As an example of process intensification, extractive dividing wall column (E-DWC) represents a combination of the two columns of the conventional extractive distillation sequence into one shell with an internal partition wall. Literature studies have reported that using an E-DWC model can reduce energy up to 51.6% (Tavan et al., 2014a) and TAC up to 35.8% (Dai et al., 2016) compared to the conventional two-column sequence of the extractive distillation process. Although E-DWC has already been used in industry (Heida et al., 2002; Diehl et al., 2005; Jobson, 2005; Parkinson, 2007; Yildirim et al., 2011; Hoyme, 2017; Staak and Grützner, 2017), the design, simulation, and control of this technology needs more investigation.

Indeed, published methods used to design an E-DWC are based either on parameters a priori suitable for the conventional model of extractive distillation with a two-column sequence or on parameters already defined by other researchers relying on different optimization methods. Midori et al. (2000) were the first to study theoretically the application of E-DWC in which the dividing wall is extended to the upper end of the column. Bravo-Bravo et al. (2010) applied a multi-objective genetic algorithm coupled with the Aspen Plus process simulator to determine the optimal design for four different column configurations. In this study, the objective of optimization was to minimize the size of both sides of the wall, the entrainer flow, and the heat duty of the sequence, under constraints of desired purities and recoveries. Kiss and al. (Kiss and Ignat, 2012; Kiss and Suszwalak, 2012; Kiss et al., 2013), have proposed a new E-DWC able to concentrate and dehydrate bio-ethanol using a heavy entrainer in a single distillation step. While varying tray numbers in an outer loop, the process operating parameters were optimized in an inner loop using the state-of-the-art SQP method, and minimizing reboiler duty. The results of the conventional two-column extractive distillation sequence simulation were used as a starting point for the E-DWC optimization. In other studies, the total annualized cost (TAC) was used as the objective

function, while the starting points for process optimization were randomly generated, obtained according to the design results of the conventional extractive distillation sequence or defined by other researchers (Xia et al., 2012; Sun et al., 2014; Tavan et al., 2014b; Tututi-Avila et al., 2014; Zhang et al., 2014, 2019, 2021 ; Loy et al., 2015; Yu et al., 2015; Wang et al., 2016; Ma et al., 2020, 2021; Waltermann et al., 2020; Ye et al., 2022; Lee et al., 2023). Review on extractive dividing wall distillation columns for separating azeotropic mixtures (Natalie et al., 2023) shows that the most of the design methods are based on the use of optimization under simulation, and the methods mentioned in this review do not represent a direct design method.

These design approaches do not fully exploit the phase equilibria knowledge that are yet essential for assessing the feasibility of distillation processes, and we intend to do so in this work for E-DWC design. For extractive distillation, well known residue curve analysis has been supplemented with volatility order regions, related to univolatility location, to assess the process feasibility, in particular for finding which component can be a distillate product, where can it leave the process, in the distillate or in the boiler (Gerbaud et al., 2019). Furthermore, computation of pinch curves in VLE diagrams gives access to limiting conditions of extractive distillation operation, in particular those related to reflux and entrainer flowrate (Brüggemann and Marquardt, 2004; Petlyuk et al., 2015), for a given expected product. As summarized in the review by Gerbaud et al. (2019), for the most common separation, namely minimum boiling azeotropic mixture A-B using a heavy entrainer E (Serafimov's class 1.0-1a), the extractive distillation process is feasible above minimum values of reflux and of entrainer flowrate. Furthermore, volatility order information states that when the univolatility curve reaches the A-E side (resp. B-E side), the distillate product is A (resp. B), corresponding to the extractive separation class (1.0-1a)-m1 (resp. (1.0-1a)-m2). (Shen et al., 2013; Gerbaud et al., 2019).

Such valuable information about phase equilibria behavior is readily tackled by using graphical tools, but this complicates the automation of conceptual design methods of extractive distillation columns. However, throughout this contribution, we propose a partial automated method implemented in VBA (Visual Basic for Applications). It is concerning the design of E-DWC. The automation of the proposed method was carried out by the implementation of a new calculation program. It takes inspiration of Petlyuk's infinitely sharp split (ISS) design method that, once a product is targeted, helps assess pinch curves from which limiting values of entrainer flow rate and reflux can be retrieved. The proposed

method is based solely on the values of phase equilibrium constant (k_i) of components along the sides of composition simplex, trajectories properties in infinitely sharp splits mode (ISS mode), and the difference point equations (DPE).

To assess the efficiency of the new design method developed in this work, the frequent case of separation of azeotropic mixtures with minimum boiling temperature in extractive distillation column using heavy entrainer where the univolatility line reaches the side A-E giving A as the distilled product (class (1.0-1a)-m1 (Serafimov, 1970; Kiva et al., 2003; Rodriguez-Donis et al., 2009) was investigated to illustrate this new method. Petlyuk et al. (2021) also studied the feasibility of the ethanol (A) – benzene (B) minimum boiling azeotrope using heavy entrainer 1-butanol where the univolatility line reaches the side B-E giving B as the distilled product (class (1.0-1a)-m2 (Serafimov, 1970; Kiva et al., 2003; Rodriguez-Donis et al., 2009). Unlike our work, Petlyuk et al., (2021) did not automated his method. In this paper, the E-DWCs, for the separation of acetone from methanol and ethanol from water using a suitable entrainer for each of the two azeotropic systems, were designed in an automated way by rigorous calculations using the VBA programming language, by calling the server Simulis Thermodynamics® (Prosim, 2023) which is presented in the form of an add-in in Excel. Design and simulation results are compared finally, a comparison with the optimization results published by other researchers for the same case study is made to assess the performance of the new method proposed in the study.

The paper is organized as follow: section 2 gives an overview of the Infinite Sharp Split method for rectifying, stripping and extractive sections encountered in a E-DWC configuration. Section 3 describes how the ISS method is used for the design of E-DWC and how one can retrieve the limiting operating parameters, namely achievable product regions, minimum entrainer flow rate and minimum reflux for each column section and how the combination of each section' information enables to assess the E-DWC feasibility. Section 4 presents a case study for two (1.0-1a)-m1 class mixtures (minimum boiling azeotrope separation using a heavy entrainer E where the univolatility curve reaches the AE side). It also compares favorably the design method and simulation results, confirming that the design method provides parameters very close to those from simulation. Conclusion in section 5 raises possible extension of the semi-automated design method to other extractive separation classes covering other azeotropic mixture separations.

2. Methods and tools

As will be shown in the design method section, the E-DWC is modelled as a composite of column sections. For given operating conditions, like tray and feed setups, reflux ratio and entrainer flow rate and product specifications, the intersection of the section's composition profiles along the column ensures the E-DWC feasibility. The design method proposed in this paper relies upon the Infinite Sharp Split method (ISS) (Petlyuk et al., 1984; Petlyuk, 1998; Petlyuk and Danilov, 1999a, 1999b, 2001a, 2001b, 2002; Tap, 2003; Petlyuk, 2004; Petlyuk et al. 2009, 2011, 2015). There exist various shortcut methods to access composition information within a column section, among which systematic algebraic methods (Levy et al., 1985), the bifurcation theory (Knapp and Doherty, 1994), or the rectification body method (Brüggemann and Marquardt, 2004). Alternatively, the ISS method enables to compute composition trajectories and pinch curves in column section on the basis of usual vapor – liquid equilibrium data with an accuracy that competes well with the other methods and has been used in particular for pinch curves in extractive sections (Petlyuk et al., 1999a, 2015, 2021, Seihoub et al., 2022, Rodriguez-Donis et al., 2023). With the help of the pinch curves, the ISS method enables the calculation of the minimum entrainer flow rate and reflux ratio in a simple way. Petlyuk et al. (2021) used his ISS method for the design of an extractive distillation process using a dividing wall column, for another separation class (1.0-1a)-m2 than we consider in this work (class (1.0-1a)-m1) and without using the difference point equations to determine trajectories in different column sections. In addition, we expressed the value of the ratio between liquid and vapor flow rates for all column sections with the same ratio. Therefore, we need to introduce and describe the ISS concepts for the reader unfamiliar with Petlyuk's works that remain confidential in the literature, despite its interest as we show.

2.1. Peculiarity of trajectories in the infinitely sharp split mode

Trajectories of different sections of a simple or extractive distillation column in the ISS mode have special characteristics. Such as the tear-off points, from which trajectories can tear off from the border towards the inside of the concentration simplex. The first automated method used for the design of an E-DWC presented in this paper was constructed with the help of these properties.

2.1.1. Simple column sections trajectories in ISS mode

Under a sharp split separation, in a simple distillation column made of a rectifying section above the main feed tray and of a stripping section below, we consider the case in which the

two products points are located on the bounding elements of the composition simplex (i.e. each product contains only a part of the feed components). We call a sharp split separation, in which the column section operates under conditions of an infinite number of trays ($N = \infty$) and finite reflux ($V/L \neq 1$), as infinitely sharp splits mode “ISS mode” (Petlyuk et al., 2011).

Trajectories of both sections in a simple distillation column at the ISS mode, where the reflux ratio is inside the interval of active reflux, are composed of two parts. The first part begins at the point of product and is located completely in the same bounding element of the composition simplex that the product point belongs to it « trunk trajectory »; i.e. the composition of the component(s) absent in the product of the presented section is equal to zero in all the points that belong to this part of the distillation trajectory. Later, in the second part, the trunk trajectory serves as a primary trajectory from which the secondary trajectory is detached from the bounding elements with dimensions higher than one, formed by the components of the product and the component(s) absent in the product (i.e. the trajectory comes inside the concentration simplex). The points which separate these two parts of the profile are called the tear-off points (x^t).

As one can see in Fig. 1, the two parts constituting the profiles of composition for a separation of ternary mixture propane (1) / n-pentane (2) / n-butane (3) at the ISS mode using a NRTL model at 1 atm, are the following:

1. a part located in the side of concentration triangle limited in its two ends by the point of bottom section product (x_B) and the tear-off point (x^t);
2. and a second part located inside concentration simplex and extends beyond the tear-off point (x^t) up to the stationary point (x^{st}), so-called the pinch point.

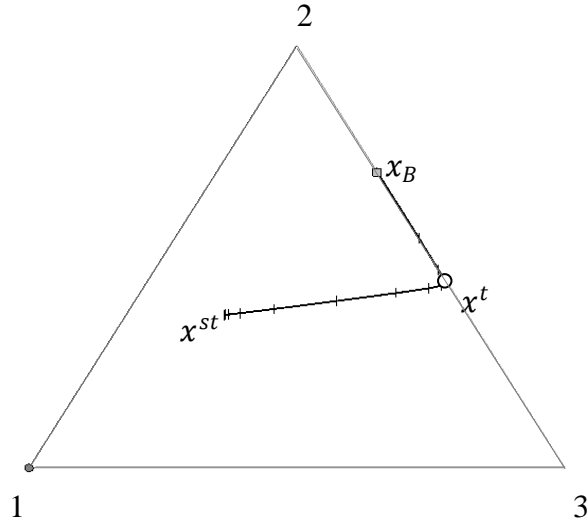


Fig. 1. Trajectories of distillation for the given product point of bottom section in the ISS mode for the ternary mixture propane (1) / n-pentane (2) / n-butane (3) and for the given reflux parameter ($V/L = 0.5$).

At a finite reflux, according to the general theory of tearing-off, the distillation trajectory tears off away from border toward the inside of the concentration simplex if some conditions are met:

1. The points of product must belong to a well-determined areas on bounding elements of concentration simplex (the product region). Petlyuk and his collaborators (Petlyuk and Danilov, 1999a; 2001b, 2002; Petlyuk, 2004; Danilov et al., 2007; Petlyuk et al., 2009, 2011, 2012) have shown that the delimitation of product regions is based on a simple conditions for the tear-off trajectories.
2. In addition, the reflux parameter L/V (resp. V/L) for the top (resp. bottom) section must exceed a so-called minimum active reflux. We note that for azeotropic mixtures the reflux parameter can also be limited by a maximum value (maximum active reflux) (Petlyuk et al., 2011). If the reflux parameter is outside the interval of active reflux, then rectifying or stripping trajectories cannot tear off toward the inside of the concentration simplex.

The two tear-off points at the minimum and maximum active reflux are called the first and second branching points, respectively. We call the set of all x^{st} points that appear inside the triangle the active segment of the first pinch branch.

The set of all the x^{st} points before the first branching point and after the second branching point and the x^t points between the first and second branching points, was named the "pinch trunk" (Petlyuk et al., 2011). After the second branching point, the segments of first pinch branch and trunk are inactive.

Fig. 2 represents a situation in which the active reflux is limited by a minimum and a maximum value. In this case of separation of the ternary azeotropic mixture (acetone (1) / chloroform (2) / benzene (3)), the tear-off theory is feasible in the limited interval of the value of the reflux parameter ($V/L \in [0.46 - 0.69]$). Therefore, tear-off of trajectories appears after the first branching point (at $V/L = 0.46$) so that the x^{st} points appear inside the triangle. For all values of the reflux parameter bigger than the maximum value in the second branching point (at $V/L = 0.69$), the trajectories cannot tear off toward the inside of the concentration simplex.

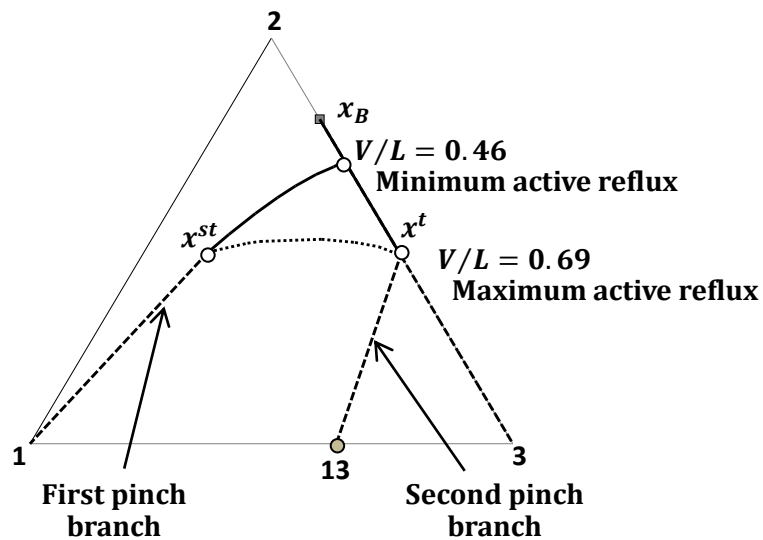


Fig. 2. Active and inactive pinch branches and interval of active reflux for the ternary mixture acetone (1) / chloroform (2) / benzene (3) using the UNIQUAC model at 1 atm.

2.1.2. Extractive section trajectories in ISS mode

In an extractive distillation column, the trajectories of the extractive section between the main feed and the entrainer feed at two different tray locations, depend not only on the reflux parameter L/V but also on the ratio E/D (entrainer flow rate / distillate rate). Under the ISS mode, if these two values are known, the pinch points can be calculated. At fixed

values of E/D and L/V , among the bundle of trajectories that have a common start and end points, the bounding trajectory of the bundle is the trajectory that passes through the saddle point S.

The bounding trajectories of the extractive section at different values of L/V and a fixed value of E/D for the separation of the system acetone (1) / water (2) / methanol (3), using a UNIQUAC model with the interaction parameters given in Table 2, are shown in Fig. 3.a. With a given value of E/D , for this system of class (1.0-1a)-m1 that is later used as a case study, the first pinch branch is the curve which brings all the saddle points at different values of L/V and is defined as that which moves toward the vertex 3 as the reflux parameter is approaching the value 1 (i.e. infinite reflux ratio). Its starting point, so-called root, is on the side 1-2. This side of the concentration simplex, where the concentration of the absent component at the top of the section is equal to zero, is called the extractive element. For reflux ratio values lower than the value corresponding to the root of the first pinch branch $(L/V)_{\min}$, the stable nodes N^+ and the saddle S will be superimposed on the extractive element. If the value of L/V is changed in the other direction ($L/V > (L/V)_{\min}$) the saddle S point leaves in the extractive element and move along the first pinch branch by increasing the value of L/V . Beyond a certain value of the reflux parameter $(L/V)_{\max}$ the stable node leaves the extractive element and moves along the second pinch branch. The second pinch branch is defined as the curve which encompasses all the stable node locations. The stable node is getting closer to the singular point of the azeotrope as the reflux ratio is approaching the infinite value. The behavior of saddle points and stable nodes of the extractive profiles and the implication on extractive process feasibility has also been described in other formalisms (Knapp and Doherty, 1994; Brüggemann and Marquardt, 2004; Rodriguez-Donis et al., 2009, Gerbaud et al., 2019).

In the case of an extractive distillation column, the locations of the pinch branches of the extractive section have a great influence on the feasibility of the separation (F. Petlyuk and Danilov, 1999; Petlyuk, 2004; Rodriguez-Donis et al., 2009; Petlyuk et al., 2015). The root of the first pinch branch moves to the top product if the value of (E/D) decreases. When the root reaches a certain limit on the extractive element corresponding to $(E/D)_{\min}$, the two pinch branches (first and second) intersect. This situation is shown in Fig. 3.b. If (E/D) still decreased, the topology of the pinch branches changes; there is no more pinch branch linking the extractive element to the opposite vertex (Brüggemann and Marquardt, 2004).

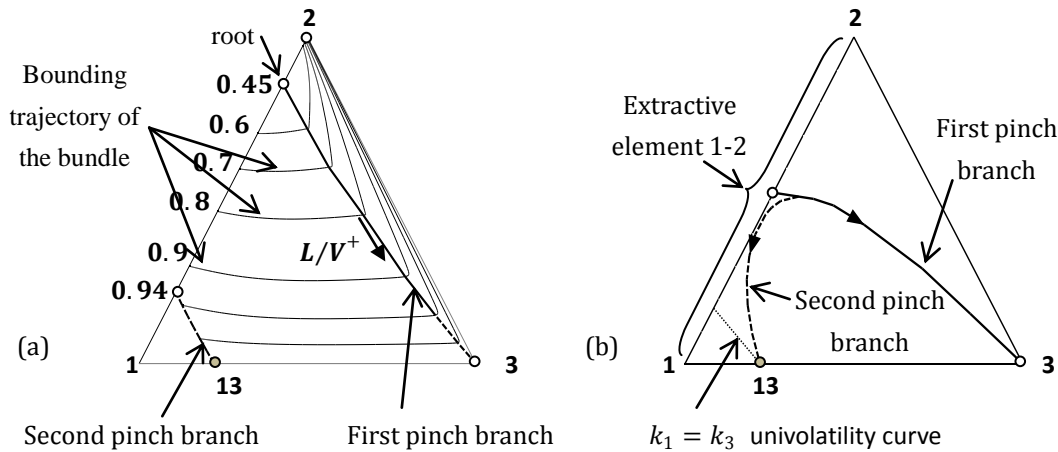


Figure. 3. Pinch branches of the extractive section for the ternary mixture acetone (1) / water (2) / methanol (3) at 1 atm for: (a) $(E/D) = 1.9$ mol/mol and (b) $(E/D)_{min}$.

It should be noted that, the ISS mode feasible operation requires a column with an infinite number of trays. In a real column with a finite number of trays, the concentration of absent(s) component(s) in products can be reduced by increasing the number of trays, and it is obviously impossible to reach a composition of the absent(s) component(s) which equal to zero. But ISS analysis is useful for finite size column operation though. From a practical point of view, it is appropriate to consider a "quasi-sharp" separation in which the column output products contain very small amounts of impurities. In this approach, we can consider the same fixed points that in the case of a ISS mode, knowing that the profiles under quasi-sharp split mode do not pass through the same stationary points of ISS mode but close to them. If separation is possible in the ISS mode, it is possible for any product purity in a finite columns (Petlyuk et al., 2012). This approach allows us to use the theory of the trajectories of distillation under the ISS mode to solve engineering problems (Petlyuk and Danilov, 2002).

Identification of feasible splits is a very important key for designing distillation process, particularly in the case of azeotropic mixtures. The first step in the proposed method is the identification of all products purities for which the design problem has a solution. Petlyuk and his collaborators (Petlyuk et al., 1984; Petlyuk, 1998; Petlyuk and Danilov, 1999a, 2001a, 2001b; Petlyuk, 2004), have shown simple relations between the feasibility of separation in ISS mode (conditions for the tear-off trajectories) and the inequalities of all components phase equilibrium coefficients k_i on bounding elements of concentration

simplex. This allows us to identify the product regions. The necessary condition for a feasible split is the location of the product points in these regions.

3. Design method

In the most commonly used design configuration for E-DWC, the wall is generally extended to the top of the column (Zhu et al., 2021) (Fig. 4a), with two vapor streams and two condensers. It should be noted that in our work, studying the (1.0-1a)-m1 extractive separation of minimum boiling azeotrope with heavy entrainer, and unlike the generally used configuration of the E-DWC (Fig. 4a), the symmetry on both sides of the wall has been waived, corresponding to Fig. 4b. Petlyuk et al., (2021) considered a similar dissymmetry for the (1.0-1a)-m2 extractive separation of the ethanol – benzene minimum boiling azeotrope with heavy entrainer 1-butanol using E-DWC. Indeed, the classical E-DWC configuration with symmetry on both sides of the wall may not correspond to the best one (Bravo-Bravo et al., 2010), even if from a manufacturing point of view, an equal number of trays would be preferred (Bravo-Bravo et al., 2010). In practical applications, this can be overcome by using packing elements with different heights (Olujić et al., 2003).

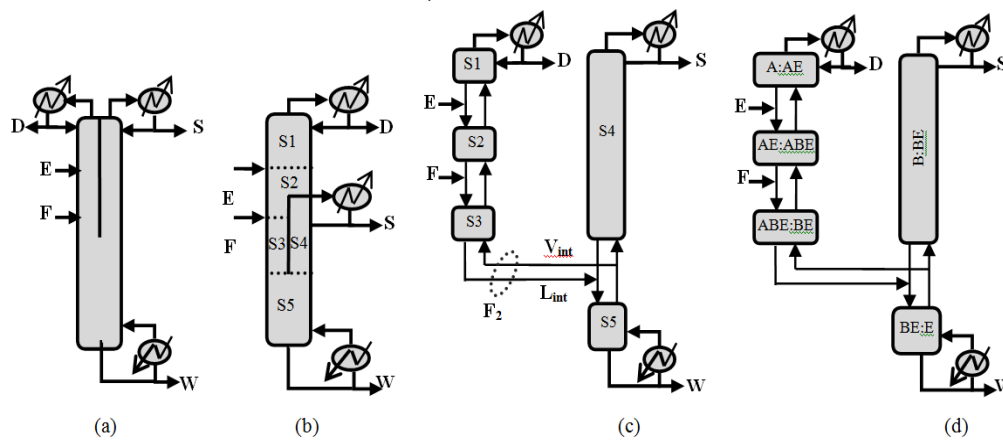


Fig. 4. Schematic diagram of (a) Most frequent E-DWC design configuration (b) E-DWC configuration in this work, (c) E-DWC design model, and (d) Separation mode in each column section.

Our configuration of the E-DWC is divided into five column sections (CSs) displayed in Fig. 4c. CSs S1, S2 and S3 approximate a classical extractive column with F being fed between S2 and S3, and the entrainer E being fed between S1 and S2. The two CSs S4 and S5 approximate the regeneration column fed by the F₂ stream. The liquid outputs from the

bottom of the two CSs S3 and S4 feed the top of CS S5. The vapor output from the top of section S5 is distributed between the two CSs S3 and S4 from the bottom, defining a vapor split ratio S_v . Fig. 4d represents the separation split in each CS of the E-DWC. For example, (AE:ABE) means that components A and E are present at the top of S2 and components A, B and E are present at the bottom of S2 that performs a sharp split separation of component B in this CS .

The procedure followed for designing E-DWC is summarized in Fig. 5. Following usual insight for (1-0-1a)-m1 extractive separation, product regions are estimated and delimited. Setting composition of feeds (z_F and x_E) and targeted final products (x_D , x_S , and x_W), as well as flow rate of the main feed (F), the entrainer flow rate will be iterated by the method until targets are matched. First, entrainer and final products flow are obtained from the material balance after having given a value to the ratio (E/D) greater than a minimum value, which limits the operation of the extractive column and that is determined by scanning the phase equilibrium coefficients values of present (k_i) and absent (k_j) components in the extractive region. Then, minimum and maximum reflux ratios in the five sections of the E-DWC are determined based only on the phase equilibrium coefficients values of (k_i) and (k_j) in each CS. A value of reflux ratio for each condenser are chosen on the condition that all CSs operate in their interval of active reflux. Finally, in order to test the feasibility of the chosen values within the limits of these operating parameters, a calculation of trajectories using the difference point equations DPEs (Holland, 2005) is carried out to check the continuity of trajectories throughout the various E-DWC sections. The number of stages in each column section is determined using the DPEs by a calculation from the bottom toward the top of the section.

As shown in Fig. 4c, in the applied design method for E-DWC, the reboiler of the extractive column in conventional sequence is replaced by a liquid (L_{int}) and vapor (V_{int}) interconnection with the regeneration column and therefore, composition and flow rates of these two streams must be defined following the procedure of the applied method.

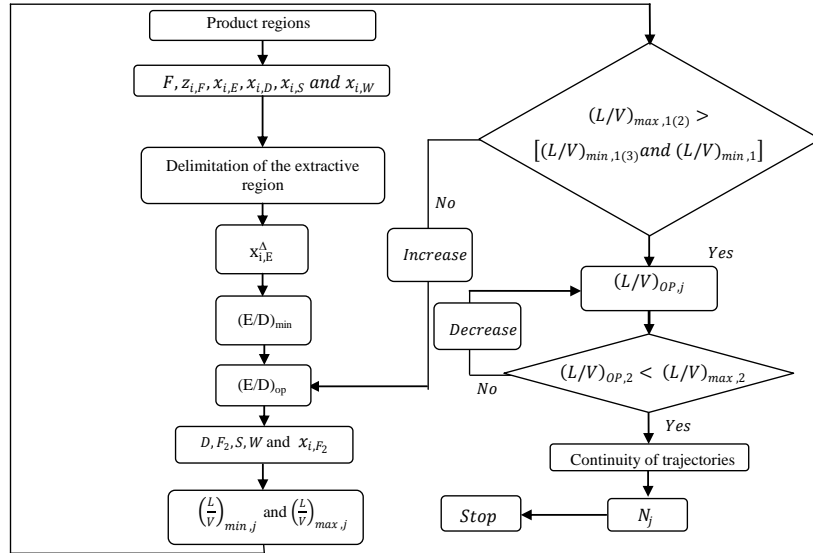


Fig. 5. Procedure applied for the design of E-DWCs used for the separation of azeotropic mixtures of type (1-0-1a)-m1.

3.1. Delimitation of operating parameters

3.1.1. Product regions

The delimitation of product regions requires a scan of phase equilibrium coefficients (k_i and k_j) of component i and j on all the considered bounding elements. Then, to determine the coordinates of product points, it is sufficient to know the coordinates of the tear-off points. At these tear-off points, the material balance equations for the considered section are satisfied both for the present(s) and the absent(s) component(s) in the product of the section. Therefore, the coordinates of the product points can be determined using the equations (1) - (3) by scanning the tear-off region determined previously (Section 2).

$$x_{i,D} = x_i^t (k_i - k_j) / (1 - k_j) \quad (\text{Top section}) \quad (1)$$

$$x_{i,W} = x_i^t (k_j - k_i) / (k_j - 1) \quad (\text{Bottom section}) \quad (2)$$

$$x_{i,(D+E)} = x_i^t (k_i - k_j) / (1 - k_j) \quad (\text{Extractive section}) \quad (3)$$

3.1.2. Minimum entrainer ratio $(E/D)_{\min}$

In the extractive section, a separation is only possible if the stable node N^+ of the extractive section is located on the extractive element and the saddle point is inside the concentration simplex. The extractive region is bounded by two points that satisfy the condition (4). Once

the two points limiting the extractive region are identified, it is necessary to determine limiting parameters of the separation in terms of entrainer flow rate and reflux ratio. The determination of these limiting parameters of the extractive column depends on the type of extractive region.

The extractive region is composed of an active and inactive region. For different (E/D) ratios, all roots representing the starting points of the first pinch branches are located inside the active extractive region. The starting points of the second pinch branches are located in the inactive extractive region. For (E/D) values lower than the minimum value, the stable nodes N^+ do not join the extractive element which means that the separation is infeasible. The determination of $(E/D)_{\min}$ is carried out automatically by mathematical formulas (Equation 6), scanning all points of the extractive region that satisfy the inequality (4). The values of $x_{i,E}^A$ are calculated by equation (5) using the phase equilibrium coefficients values considering that each point of the extractive region is the root of the first or the second pinch branch. A scan of all the values of (E/D) determined in each point of the extractive region gives the minimum value.

$$k_{iD}^t > k_j^t > k_{iE}^t \quad (4)$$

$$x_{i,E}^A = x_i^t (k_i^t - k_j^t) / (1 - k_j^t) \quad (5)$$

$$E/D = (x_{iD,E}^A - x_{iD,D}) / (x_{iD,E}^A - x_{iD,E}) \quad (6)$$

3.1.3. Reflux ratios

a. Column section S1

In the rectification section of the left side of the wall (S1), feasibility implies that S1 trajectories intersect with trajectories of section (S2) in the extractive element. But it is impossible that the stable points N^+ of the extractive section trajectories exceed the point of the univolatility curve located in the extractive element. Therefore, the intersection of these two sections trajectories is met when the profile of the rectification section exceeds this point of the univolatility curve. The first value of (L/V) which satisfies this condition is the minimum value $(L/V)_{\min}$. The determination of this minimum value requires:

- 1- First, the calculation of the coordinates of the intersection point of univolatility curve with the extractive element; their determination is carried out automatically by

mathematical formulas based on the values of the phase equilibrium coefficients on the extractive element.

2- Second, the identification of the stationary points (N^+) of S1 trajectories using the DPE of the rectifying section.

b. Column section S2

Each (E/D) value has two limits' values for the reflux ratio $(L/V)_{min}$ and $(L/V)_{max}$ (see Fig. 2). Beyond these two values, no trajectories of the extractive section join the extractive element. This implies that it is impossible to have trajectories linking the two CSs S1 and S2. The two limit values are calculated using the phase equilibrium coefficient of the absent component in the first and second branching points using Eq. 7. Each value of (E/D) corresponds to two values of x_i^t which represents the case of trajectories where the stable and the saddle points were superposed; one of these two points corresponds to $(L/V)_{min}$ from which trajectories of the extractive section tear off the extractive element and move toward the inside of the composition simplex (the root of the first pinch branch) and the other corresponds to $(L/V)_{max}$ from which stable points move from the side AE toward the univolatility curve (the root of the second pinch branch). Determination of these two values requires the selection of an operating value of (E/D) higher than $(E/D)_{min}$.

$$(L/V)_{min,2} = k_j^{t(1)} \quad \text{and} \quad (L/V)_{max,2} = k_j^{t(2)} \quad (7)$$

c. Column section S3

For the calculation of the trajectory of CS S3, constructed from bottom to top, the starting point (x_{i,F_2}) , located in the product region of this section, is obtained by assuming a partial reboiler in the bottom of the section. For a feasible design, trajectories of this CS and of CS S2 have to intersect. It is evident that the intersection point of these two CSs trajectories is located inside concentration simplex. Therefore, as a first feasibility criterion in this CS, it is necessary to determine the value of (V/L) which corresponds to the first branching point $((V/L)_{min,3})$; this means that beyond this value we can have trajectories that pass from the product region to the internal space of the composition simplex.

$(V/L)_{min,3}$ is determined by Eq. 9. The value of k_j^t corresponds to the first tear-off point for fixed product composition. The composition at the first branching point (x_i^t) is identified automatically by a systematic calculation using Eq. 8.

$$x_{i,F_2} = x_i^t (k_j^t - k_1^t)/(k_j^t - 1) \quad (8)$$

$$(V/L)_{min,3} = k_j^t \quad (9)$$

d. Column section S4 and S5

From the trajectories calculation based on the DPE for a rectifying and a stripping CS, we can determine the minimum value of the ratio between the liquid and the vapor flow rate, from which trajectories arrive or exceed the composition point equivalent to the feed of these two sections (x_{i,F_2}).

3.2. Feasibility evaluation of the chosen parameters

In the chosen configuration for the E-DWC (Fig. 4 c) two condensers are used, and therefore two sources of reflux are present. The selection of operating reflux ratio corresponding to each condenser is then carried out in a way to ensure the best operation of each CS.

As a first step, we expressed the value of the ratio between liquid and vapor flow rates for all CSs with the same ratio; that of CS S1 for the left side of the wall (Eqs. 10, 11 and 12) and that of the CS S4 (Eq. 13) for the right side of the wall. This link of the different CSs is primary in order to automate the proposed method.

$$(L/V)_{min,1(2)} = \left(k_{j(2)}^{t(1)} - (E/D) \right) / (1 - (E/D)) \quad (10)$$

$$(L/V)_{max,1(2)} = \left(k_{j(2)}^{t(2)} - (E/D) \right) / (1 - (E/D)) \quad (11)$$

$$(L/V)_{min,1(3)} = k_{j(3)}^t - \left(\frac{E+F}{L_{int}-V_{int}} (k_{j(3)}^t - 1) \right) \quad (12)$$

$$(L/V)_{min,4(5)} = \left(k_{j(5)}^{st} - \left(L_{int}/W (k_{j(5)}^{st} - 1) \right) \right) / \left(1 - \left(V_{int}/W (k_{j(5)}^{st} - 1) \right) \right) \quad (13)$$

Where $(L/V)_{min,k(j)}$ is the value of the ratio (L/V) of the CS k defined by the minimum value of this parameter in the CS j . $k_{j(2)}^{t(1)}$ and $k_{j(2)}^{t(2)}$ are respectively, the phase equilibrium coefficients of the absent component j in the root of the first and the second pinch branch in the extractive section (S2). $k_{j(3)}^t$ is the phase equilibrium coefficients of the absent component in the first tear-off point of the CS 3. $k_{j(5)}^{st}$ is the phase equilibrium coefficients of the absent component in the stationary point of the CS S5 trajectory at minimum reflux.

Calculation of $(L/V)_{min,4(5)}$ requires the flow rates of L_{int} and V_{int} , their identification imposes to give a value to the CS S1 reflux.

In the chosen configuration for the E-DWC, the first condenser located at the top of CS S1 covers the needs in liquid of the CSs S1, S2 and S3. Also, part of the CS S5 liquid comes from the bottom of the CS S3. The second condenser covers the needs in the liquid of the CSs S4 and S5. The right choice of these two reflux (Eqs. 14 and 15) allows us to reach the best performance in all CSs. Once the two reflux values are set, liquid and vapor flow rates in each CS of the E-DWC will be simply calculated using material balance equations.

$$R_1 = \left[\left(\max (L/V)_{min,1(j)} \right) / \left(1 - \max (L/V)_{min,1(j)} \right) \right] \times a \quad \text{With } j = 1,2 \text{ et } 3 \quad (14)$$

$$R_4 = \left[\left(\max (L/V)_{min,4(j)} \right) / \left(1 - \max (L/V)_{min,4(j)} \right) \right] \times a \quad \text{With } j = 4 \text{ et } 5 \quad (15)$$

Despite that the only condition for the existence of a bundle of trajectories in a CS is the location of product point in the product region, this condition is not sufficient to confirm the feasibility of separation for the whole E-DWC where there must be a continuity of trajectories of the five CSs of the E-DWC (condition of sections joining). Trajectories of the extractive (S2), stripping (S3 and S5) and rectifying (S1 and S4) CSs can be plotted using the DPE appropriate to each type of CS.

In this work a new DPE for the calculation of the extractive section trajectories is developed (Eq. 16). The equation has been established by applying a material balance around the two combined rectifying and extractive CSs.

$$\frac{dx}{dn} = \left(\frac{1}{R_\Delta} + 1 \right) [x - y^*] + \frac{1}{R_\Delta} [X_\Delta - x] \quad (16)$$

$$X_\Delta = (x_{i,D} - (E/D) x_{i,E}) / (1 - (E/D)) \quad (17)$$

$$R_\Delta = (R_1 + (E/D)) / (1 - (E/D)) \quad (18)$$

In Petlyuk et al. (2021), no equivalent to Eq. 16 was proposed. For the extractive section, the tray-to-tray calculation is carried out from the bottom upward until reaching their respective stable nodes

In the E-DWC, for the trajectories calculation of the CSs S3, S4, and S5, as well as to initialize the rigorous simulation, it is necessary to define the composition of the two interconnecting streams V_{int} and L_{int} . The determination of the composition of these streams is performed after setting the operating parameters of entrainer and reflux ratio associated with each condenser. Trajectory of CS S5 can be calculated by a systematic

calculation using the DPE for a stripping CS. The liquid composition which exceeds the value of the composition equivalent to the bottom product of the CS S3 calculated by the material balance (assuming a partial reboiler) represents the composition of the interconnecting liquid stream. This composition is the first point from which trajectories calculation of the two CSs S3 and S4 are executed.

After finding operating parameters ensuring the process feasibility via the intersection of the different CSs profiles, the tray number of each CS is calculated subsequently using the DPE. The integration begins in all sections from the bottom to the top. Without this final precaution, the presentation of the components composition on each tray of the CS will not be accurate (Lucia et al., 2008).

4. Design method validation

In our work, the design method is automated using the VBA programming language, by calling the thermodynamic property server Simulis Thermodynamics® (Prosim, 2023) which is presented in the form of an add-in in Excel, and gives access to a library of components, of thermodynamic models and of phase equilibria calculation routines. The objective of the automation is to reduce significantly the complexity and the time that must be devoted to the determination of the operating and design parameters. The typical time for solving a single case study is one min on a windows laptop with a 1.8 GHz processor and 4 GB RAM.

The two case studies are detailed in section 4.1. The parameters determined by this new design method are presented in section 4.2. Executing the program coded in VBA provides as a result all the necessary conditions to initialize a rigorous simulation, which can further help engineers for refining design, optimization and control configuration of the E-DWC. In section 4.3, a comparison, in terms of products purities and interconnection streams composition, between E-DWC processes designed via our design method and those completed using rigorous simulation in ProSim Plus® (Prosim, 2023) where the design parameters are used as initial parameters. Splitting the E-DWC in "sub-columns" interconnected, as presented in Fig. 4c, was used to simulate the system. A comparison with other simulated literature results is given in section 4.4.

4.1. Case Studies

Systems investigated in this work, acetone (A) / methanol (B) / water (E) and ethanol (A) / water (B) / ethylene glycol (E), belong to the class (1.0-1a)-m1 corresponding to the

extractive separation of a minimum boiling temperature azeotrope using a heavy entrainer where the univolatility line reaches the side AE giving A as the distilled product. Note that Petlyuk et al., 2021 studied the E-DWC for a case study belonging to class (1.0-1a)-m2 where (B) is the distillate product. The first case is the separation of the acetone / methanol azeotropic system with water as a heavy entrainer. According to the statistics in the supplementary material of Gerbaud's review, more than 30 papers in the extractive distillation literature have studied this separation (Gerbaud et al., 2019) . Table 1 shows UNIQUAC binary interaction parameters taken from the Aspen Plus database for the liquid-vapor equilibrium calculation while the vapor phase is considered as an ideal gas. Azeotrope prediction, 77.7 mol. % acetone at 328.39 K agrees with experimental values 78.3 mol. % acetone at 328.55 K.

The second case is the separation of the ethanol / water azeotropic system. The most commonly used entrainer for breaking this azeotrope is ethylene glycol (Gerbaud et al., 2019). The NRTL model is used to describe the non-ideality of the liquid phase, and the vapor phase is supposed to be an ideal gas. Table 1 shows the binary interaction parameters determined by regression using experimental data (Guella and Bernaoui, 2017). Azeotrope prediction, 91.6 %mol ethanol at 351.38 K agrees with experimental values 90.4 %mol ethanol at 351.35 K.

Table 1. Binary interaction parameters of UNIQUAC model for acetone / methanol / water and NRTL model for ethanol / water / ethylene glycol systems.

| Binary | acetone / methanol | acetone / water | methanol / water |
|-----------------|--------------------|---------------------------|-------------------------|
| A_{ij0} | -225.153 | -3122.58 | 432.8785 |
| A_{ji0} | 52.7705 | 1612.196 | -322.131 |
| A_{ijT} | 0 | 8.6051 | -1.0662 |
| A_{jiT} | 0 | -4.8338 | 0.6437 |
| Binary | ethanol / water | ethanol / ethylene glycol | water / ethylene glycol |
| A_{ij0} | -120.615 | 819.825 | 49.55 |
| A_{ji0} | 1344.69 | 261.014 | -41.13 |
| $a_{ij}=a_{ji}$ | 0.3 | 0.331 | 0.3 |

Fig. 6 shows the residue curve maps and univolatility curve for both ternary mixtures A-B-E. For both mixtures, the univolatility curves reaches the A-E side, corresponding to the

(1.0-1a)-m1 extractive separation class (Gerbaud et al. 2019) where A is the distilled product.

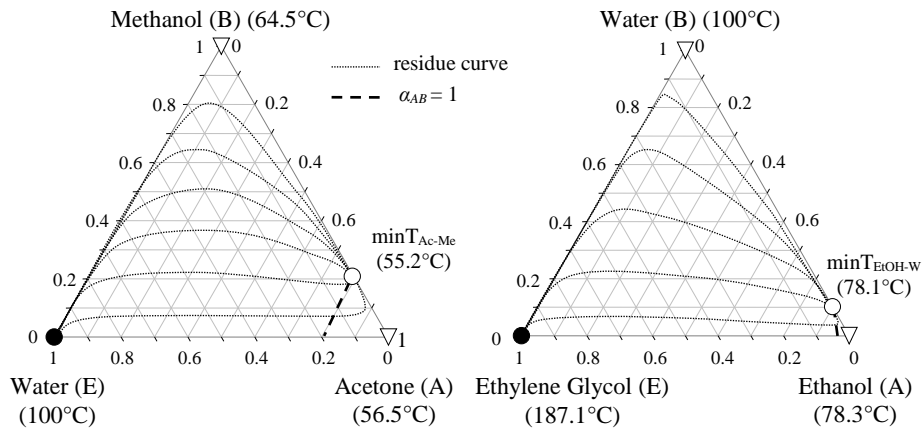


Fig. 6. Residue curve maps and univolatility curve for the acetone (A) – methanol (B) – water (E) and ethanol (A) – water (B) – ethylene glycol (E) mixtures.

Feed conditions of the studied systems M1 acetone (A) / methanol (B) / water (E) and M2 and ethanol (A) / water (B) / ethylene glycol (E) are summarized in Table 2. Entrainer is fed pure. No entrainer recycling is considered. Products purities are 99.98 %mol. A-B mixture and entrainer are fed as a saturated liquid.

Table 2. Feed conditions and products purity of the two systems studied.

| A / B / E | $z_{A,F}/z_{B,F}$ | $z_{E,E}$ | P (atm) | F (kmol/hr) | $x_{A,D} = x_{B,S} = x_{E,W}$ |
|--------------------------------------|-------------------|-----------|---------|-------------|-------------------------------|
| M1 acetone / methanol / water | 0.5 / 0.5 | 1 | 1 | 540 | 0.9998 |
| M2 ethanol / water / ethylene glycol | 0.85 / 0.15 | | | 100 | |

4.2. Design method parameters

The design and operation parameters determined by the design method for separating the mixtures M1 and M2 in an E-DWC, are summarized in Tables 3 and 4. Table 3 displays the minimum values of entrainer flow rate and reflux ratios.

Table 3. Minimum values of entrainer flow rate and reflux ratios.

| | $(E/D)_{\min}$ | $R_{1,\min}$ | $R_{2,\min}$ |
|-----------------------------------|----------------|--------------|--------------|
| acetone / methanol / water | 0.95 | 2.87 | 1.08 |
| ethanol / water / ethylene glycol | 0.5 | 0.43 | 0.39 |

Table 4 displays all the design parameters for achieving the product purities listed in Table 2. Entrainer and products flow, shown in Table 4, are obtained from the material balance

after having selected a value to the ratio (E/D) greater than the minimum value, $1.9 > 0.95$. and $0.99 > 0.5$ for mixture M1 and M2 respectively. One notices that the design values of reflux listed in Table 4 are greater than the minimum value in Table 3

Table 4. Design method results for the separation of acetone / methanol / water and ethanol / water / ethylene glycol in an E-DWC.

| Systems | N_1 | N_E | N_F | N_4 | N_5 | E (kmol/h) | D (kmol/h) | S (kmol/h) | W (kmol/h) | V_{int} (kmol/h) | R_1 | R_2 | S_V |
|---------------------|-------|-------|-------|-------|-------|---------------|---------------|---------------|---------------|-----------------------|-------|-------|-------|
| Acetone (A) | | | | | | | | | | | | | |
| Methanol (B) | 66 | 25 | 53 | 25 | 5 | 514.24 | 269.98 | 270.03 | 514.23 | 1124.9 | 3.16 | 1.19 | 0.65 |
| Water (E) | | | | | | | | | | | | | |
| Ethanol (A) | | | | | | | | | | | | | |
| Water (B) | 34 | 3 | 28 | 5 | 3 | 84.7 | 85.01 | 14.99 | 84.7 | 139.56 | 0.64 | 0.43 | 0.86 |
| Ethylene glycol (E) | | | | | | | | | | | | | |

Firstly we check the relevance of the minimum entrainer rate value by analyzing the location of the stable nodes (N^+) of the extractive CS trajectories, for $0 < L/V < 1$ (Fig. 7).

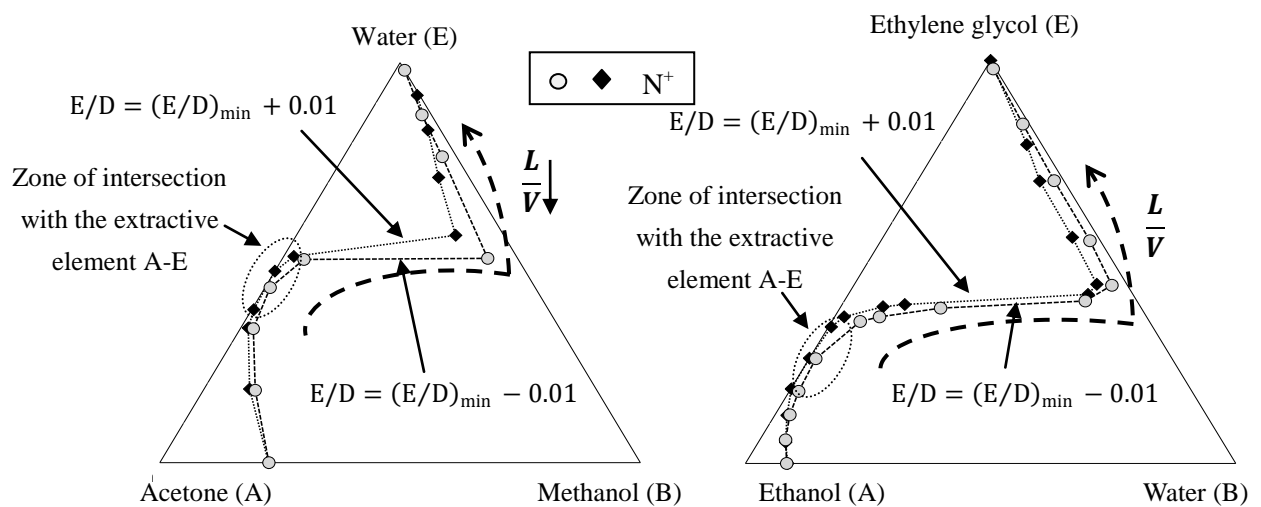


Fig. 7. Stable Nodes of the Extractive CS Trajectories for Different (L/V) Values of the M1 and M2 Case Studies.

In Fig. 7, the stable node N^+ corresponds to the pinch points of the extractive CS trajectories determined by varying the reflux rate. When $E/D < (E/D)_{min}$, regardless of the reflux value, N^+ cannot join the extractive element that lies on the A-E side of the triangle, which implies that separation is not feasible since there is no intersection between the extractive

section trajectory and the rectifying section trajectory that enables to reach the expected distillate product.

The next step is to check by simulation whether the design parameters listed in Table 4, effectively allow to obtain desired products with the specified purity.

4.3. Rigorous simulation based on design parameters

Simulations are carried out using process simulator ProSim Plus® (Prosim, 2023) with the design parameters listed in Table 4 used as initial parameters. The results, obtained by implementing the design method parameters in rigorous simulation, are shown in Table 5.

Table 5. Products purities and interconnection streams composition obtained by design method and rigorous simulation.

| | | $x_{B,Vint}$ | $x_{E,Vint}$ | $x_{B,Lint}$ | $x_{E,Lint}$ | $x_{A,D}$ | $x_{B,S}$ | $x_{E,W}$ |
|---------------------|---------------------|--------------|--------------|--------------|--------------|-----------|-----------|-----------|
| Acetone (A) | Shortcut design | 0.8065 | 0.1935 | 0.6164 | 0.3833 | 0.9998 | 0.9998 | 0.9998 |
| Methanol (B) | | | | | | | | |
| Water (E) | Rigorous simulation | 0.8262 | 0.1718 | 0.6282 | 0.3701 | 0.9965 | 0.9963 | 0.9985 |
| Ethanol (A) | Shortcut design | 0.9571 | 0.0429 | 0.6202 | 0.3789 | 0.9998 | 0.9998 | 0.9998 |
| Water (B) | | | | | | | | |
| Ethylene glycol (E) | Rigorous simulation | 0.9081 | 0.0902 | 0.5925 | 0.4064 | 0.9995 | 0.9977 | 0.9995 |

It can be seen that for both mixtures, rigorous simulation leads to products and interconnection streams purity specifications close to those imposed in the design method. Slight differences are expected due to the infinite split hypothesis of the design method that is not verified in the simulation. These results prove the reliability and accuracy of the new method.

The analysis of trajectories, along the sections representing the E-DWC, presented in Fig. 8, confirm that the column operates above its minimum entrainer flowrate and reflux parameters listed in Table 3. In the extractive CS S2, the composition of the absent component reaches almost zero value near the concentration section; this implies that the trajectory of this CS joins the extractive region in the top and that the CS has enough stages to join the extractive element where the extractive CS S2 profile can intersect with the rectifying profile of CS S1 that ends at the top distillate product point. In addition, the number of trays in each section is sufficient to ensure the best operation with stable

composition in the ends of the second column and at the top of the first column. All this confirms the precision of the proposed method.

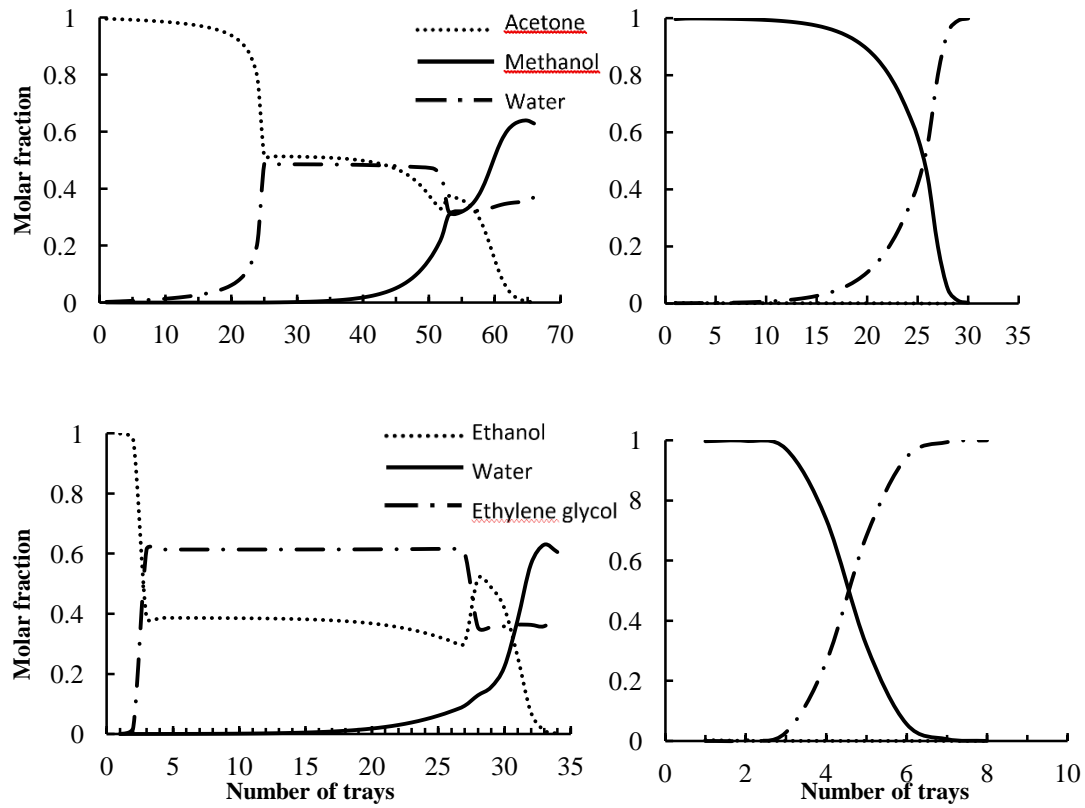


Fig. 8. Composition trajectories obtained by the rigorous simulation in the E-DWC for: (a) CSs S1, S2 and S3; (b) CSs S4 and S5.

Fig. 9 displays the column trajectories obtained by the rigorous simulation and those calculated by the design method. Profiles are sharper for the design method, in coherence with the infinite sharp split hypothesis. Overall, the agreement is remarkable, and this confirms the precision of the proposed design method.

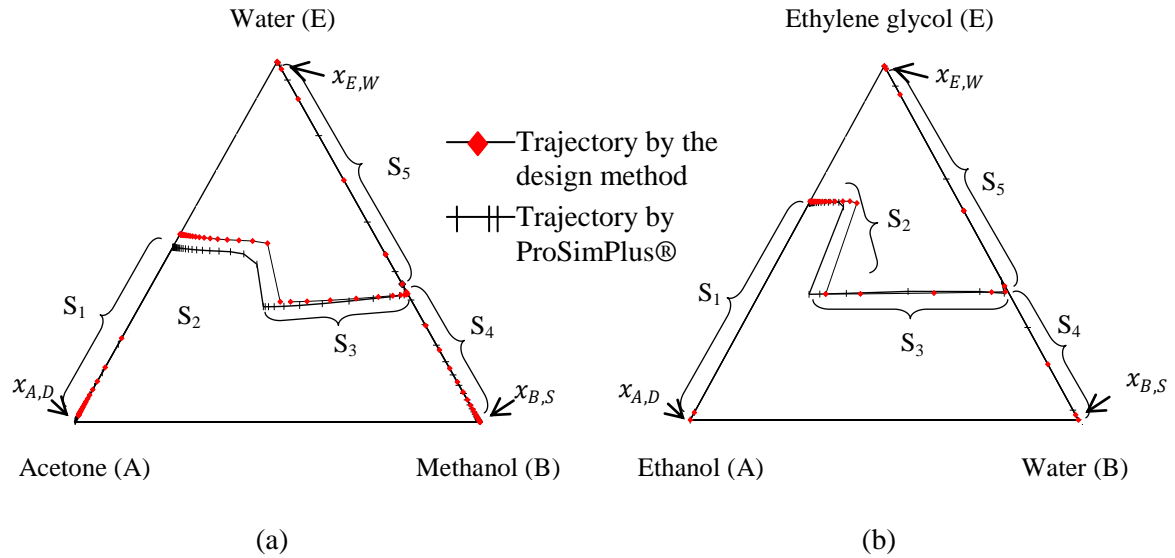


Fig. 9. Composition trajectories in the E-DWC obtained by the rigorous simulation and calculated by the design method for the systems: (a) acetone / methanol / water, (b) ethanol / water / ethylene glycol.

4.4. Comparison with conventional extractive distillation process and E-DWC literature results

All mixture separations have been studied by using a classical extractive distillation column – regeneration column sequence, for the same product purity and recovery and one compares it with the E-DWC process. Results are displayed in Table 6.

Table 6. Comparison of conventional extractive distillation process and E-DWC process simulation.

| Systems | Parameters | Conventional ED process | E-DWC |
|-----------------------------|------------------|-------------------------|------------------|
| Acetone (A) Methanol (B) | R_1 | 4.02 | 3.16 |
| | R_2 | 1.36 | 1.19 |
| Water (E) | F_E (kmol/h) | 514.24 | |
| | Q_{total} (kW) | 17413.9 | 17094.8 (-1.83%) |
| Ethanol (A) Water (B) | R_1 | 0.73 | 0.64 |
| | R_2 | 0.87 | 0.43 |
| Ethylene glycol (E) | F_E (kmol/h) | 84.7 | |
| | Q_{total} (kW) | 2569.3 | 2249.4 (-12.45%) |

Table 6 shows that, for the same entrainer flow rate, the E-DWC energy consumption is lower, marginally for the separation of acetone – methanol with water but up to -12% for the

separation of ethanol – water with ethylene glycol. This reduction is mainly due to the prevention of unnecessary energy waste due to the remixing effect located in the stripping section of the classical extractive distillation column.

In addition to this reduction in energy consumption, the compacting of two columns into one shell in the EDWC is another advantage that provides a saving in the required installation space.

In Table 7, we also compare our simulation results initialized by our design method and those obtained by other studies with E-DWC, that have achieved the results by optimization, and not using any design method like we do. The two literature studies were selected on the basis that they use the same conditions of the main feed in terms of flow rate and composition, almost the same specifications of product purities, and the same entrainer composition. For the separation of acetone – methanol with water, the study proposed by Wu et al. (2013) was chosen and for the separation of ethanol – water with ethylene glycol, the study proposed by Aurangzeb and Jana (2019) was selected.

Table 7. Comparison between the results obtained by the implementation of our design method and those obtained by other studies (Wu et al., 2013, Aurangzeb and Jana, 2019).

| Mixtures | acetone/methanol/water | | ethanol/water/ethylene glycol | |
|-------------------|------------------------|-----------|-------------------------------|-----------|
| | Wu et al. (2013) | this work | Aurangzeb and Jana (2019) | this work |
| P (atm) | 1 | 1 | 1 | 1 |
| F (kmol/hr) | 540 | 540 | 100 | 100 |
| $z_{A,F}/z_{B,F}$ | 0.5/0.5 | 0.5/0.5 | 0.85/0.15 | 0.85/0.15 |
| E (kmol/hr) | 1100.00 | 514.24 | 88.94 | 84.70 |
| $z_{E,E}$ | 1 | 1 | 1 | 1 |
| N_1 | 25 | 25 | 4 | 3 |
| N_2 | 15 | 28 | 19 | 25 |
| N_3 | 17 | 13 | 10 | 6 |
| N_4 | 58 | 25 | 24 | 5 |
| N_5 | 12 | 5 | 6 | 3 |
| S_V | 0.68 | 0.65 | 0.835 | 0.86 |
| $x_{A,D}$ | 0.9940 | 0.9965 | 0.9981 | 0.9995 |
| $x_{B,S}$ | 0.9950 | 0.9963 | 0.9990 | 0.9977 |
| $x_{E,W}$ | 0.9995 | 0.9985 | 1 | 0.9995 |
| R_1 | 3.323 | 3.160 | 0.340 | 0.640 |

| | | | | |
|------------|----------|----------|---------|---------|
| R_2 | 0.8807 | 1.190 | 0.242 | 0.430 |
| Q_C (kW) | 14610.15 | 16469.30 | 1498.20 | 1717.87 |
| Q_B (kW) | 16284.60 | 17094.80 | 2018.24 | 2249.38 |

As can be seen, for the separation of acetone – methanol using water, the simulated design proposed by Wu et al. (2013) uses a solvent flow rate much higher than that determined by our design method. With nearly half their entrainer flowrate and much less trays in sections S4 and S5, we can reach almost the same purity of the final products. As common in distillation, less trays and a slightly larger reflux flowrate for the same purity explains the difference in energy consumption which is higher for our design. Notice that Wu et al. (2013) optimized energy consumption and that our design method does not includes that consideration.

For the separation of ethanol – water with ethylene glycol, the EDWC optimization results published by Aurangzeb and Jana (2019) show that the solvent flow rate, the purity of the final products, and the number of stages in sections S1, S2 and S3 are very close to the values found by our design method proposed in this article. The two sections S4 and S5 of Aurangzeb and Jana (2019) are much bigger than us, but they have stricter and nearly pure product specifications than us. On the other hand, their optimized energy consumption is lower than us, due to the same comment than above with Wu’s work (Wu et al., 2013).

Values of the vapor split are close between our design and their optimal operation, another credit to our design method relevance. Notice that S_v value greater than 0.5 means that the extractive side (S1-S3) of the E-DWC needs more vapor flow and therefore a larger share of the boiler heat duty.

5. Conclusion

The objective of the presented work was to establish a fully automated and general design methodology for the separation of azeotropic mixtures of type (1-0-1a)-m1 in an E-DWC. The proposed design method is executed by rigorous calculations using the VBA programming language and by calling the server for thermophysical properties and phase equilibria calculations " Simulis Thermodynamics". It is based solely on mathematical formulas; without the need to go through the graphical presentations that are needed due to the non-ideal behavior of azeotropic mixtures. This method of design has proved to be very useful for designing systematically and rapidly an E-DWC, with a low effort of calculation, based only on the properties of the ISS separation mode, the equilibrium constants values of mixture components in the sides of composition simplex, and the DPEs.

The separation of acetone from methanol and ethanol from water using a suitable entrainer for each of the two azeotropic systems has been investigated to validate the proposed model. The obtained results of the rigorous simulation using ProSim Plus proved the reliability and the precision of this new design method.

The comparison with the optimization results published by other researchers proves that this new design method leads to results close to those found after optimization.

The program of rigorous calculations representing the new design method described in this paper is generalized to the separation of all azeotropic mixtures that belong to the class (1-0-1a)-m1. In our next works, this calculation program will be generalized to different types of azeotropic mixtures.

ORCID

Fatima Zohra SEIHOUB <https://orcid.org/0000-0003-1932-1405>

Vincent GERBAUD <https://orcid.org/0000-0003-2738-7922>

Hassiba BENYOUNES <https://orcid.org/0000-0002-5283-8177>

References

- Aniya, V., De, D., Singh, A., Satyavathi, B., 2018. Design and operation of extractive distillation systems using different class of entrainers for the production of fuel grade tert-butyl Alcohol: A techno-economic assessment. *Energy* 144, 1013–1025. <https://doi.org/10.1016/j.energy.2017.12.099>
- Aurangzeb, M., Jana, A.K. A., 2019. Novel Heat Integrated Extractive Dividing Wall Column for Ethanol Dehydration. *Ind. Eng. Chem. Res.* 58(21), 9109-9117. <https://doi.org/10.1021/acs.iecr.9b00988>
- Bravo-Bravo, C., Segovia-Hernández, J.G., Gutiérrez-Antonio, C., Durán, A.L., Bonilla-Petriciolet, A., Briones-Ramírez, A., 2010. Extractive Dividing Wall Column: Design and Optimization. *Ind. Eng. Chem. Res.* 49, 3672–3688. <https://doi.org/10.1021/ie9006936>
- Brüggemann, S., Marquardt, W., 2004. Shortcut methods for nonideal multicomponent distillation: 3. Extractive distillation columns. *AIChE J.* 50, 1129–1149. <https://doi.org/10.1002/aic.10108>
- Dai, X., Ye, Q., Qin, J., Yu, H., Suo, X., Li, R., 2016. Energy-saving dividing-wall column design and control for benzene extraction distillation via mixed entrainer. *Chem. Eng. Process. Process*

- Intensif. 100, 49–64. <https://doi.org/10.1016/j.cep.2015.11.014>
- Danilov, R.Y., Petlyuk, F.B., Serafimov, L. a., 2007. Minimum-reflux regime of simple distillation columns. *Theor. Found. Chem. Eng.* 41, 371–383. <https://doi.org/10.1134/S0040579507040069>
- Diehl, T., Kolbe, B., Gehrke, H., 2005. Uhde Morphylane® extractive distillation where do we stand? pp. 1–12.
- Gerbaud, V., Rodriguez-Donis, I., Lang, P., Denes, F., Hegely, L., You, X., 2019. Review of Extractive Distillation: process design, operation optimization and control. *Chem. Eng. Res. Des.*, 141, 229-271. <https://doi.org/10.1016/j.cherd.2018.09.020>
- Guella, F., Bernaoui, A., 2017. Conception de procédé de distillation extractive du mélange éthanol - eau en présence des liquides ioniques. Université des Sciences et de la Technologie d'Oran-MB.
- Heida, B., Bohner, G., Kindler, K., 2002. Consider divided-wall technology for butadiene extraction. *Hydrocarb. Process.* 81, 50B–50H.
- Holland, S.T., 2005. Column profile maps: A tool for design and analysis of complex distillation systems. School of Chemical and Metallurgical Engineering.
- Hoyme, C.A., 2017. Dividing Wall Columns in the Chemical Industry., In *Handboo.* ed. Springer, Cham.
- Jobson, M., 2005. Dividing wall distillation comes of age. *Chem. Eng.* 766, 30–31.
- Kiss, A.A., Ignat, R.M., 2012. Innovative single step bioethanol dehydration in an extractive dividing-wall column. *Sep. Purif. Technol.* 98, 290–297. <https://doi.org/10.1016/j.seppur.2012.06.029>
- Kiss, A.A., Suszwalak, D.J.-. P.C., 2012. Enhanced bioethanol dehydration by extractive and azeotropic distillation in dividing-wall columns. *Sep. Purif. Technol.* 86, 70–78. <https://doi.org/10.1016/j.seppur.2011.10.022>
- Kiss, A.A., Suszwalak, D.J.-P.C., Ignat, R.M., 2013. Breaking azeotropes by azeotropic and extractive distillation in a dividing-wall column. *Chem. Eng. Trans.* 35, 1279–1284. <https://doi.org/10.3303/CET1335213>
- Kiva, V.N., Hilmen, E.K., Skogestad, S., 2003. Azeotropic phase equilibrium diagrams: a survey. *Chem. Eng. Sci.* 58, 1903–1953. [https://doi.org/10.1016/S0009-2509\(03\)00018-6](https://doi.org/10.1016/S0009-2509(03)00018-6)

- Knapp, J.P., Doherty, M.F., 1994. Minimum entrainer flows for extractive distillation: A bifurcation theoretic approach. *AIChE J.* 40, 243-268. <https://doi.org/10.1002/aic.690400206>
- Lei, Z., Li, C., Chen, B., 2003. Extractive Distillation: A Review. *Sep. Purif. Rev.* 32, 121–213. <https://doi.org/10.1081/SPM-120026627>
- Levy, S.G., Van Dongen, D.B., Doherty, M.F., 1985. Design and synthesis of homogeneous azeotropic distillations. 2. Minimum reflux calculations for nonideal and azeotropic columns. *Ind. Eng. Chem. Fundam.* 24(4), 463-474.
- Loy, Y.Y., Lee, X.L., Rangaiah, G.P., 2015. Bioethanol recovery and purification using extractive dividing-wall column and pressure swing adsorption: An economic comparison after heat integration and optimization. *Sep. Purif. Technol.* 149, 413–427. <https://doi.org/10.1016/j.seppur.2015.06.007>
- Lucia, A., Amale, A., Taylor, R., 2008. Distillation pinch points and more. *Comput. Chem. Eng.* 32, 1350–1372. <https://doi.org/10.1016/j.compchemeng.2007.06.019>
- Ma, Y., McLaughlan, M., Zhang, N., Li, J., 2020. Novel feasible path optimisation algorithms using steady-state and/or pseudo-transient simulations. *Comput. Chem. Eng.* 143, 107058. <https://doi.org/10.1016/j.compchemeng.2020.107058>
- Ma, Y., Zhang, N., Li, J., Cao, C., 2021. Optimal design of extractive dividing-wall column using an efficient equation-oriented approach. *Front. Chem. Sci. Eng.* 15, 72–89. <https://doi.org/10.1007/s11705-020-1977-y>
- Midori, S., Shuang Ning Zheng, Yamada, I., 2000. Analysis of divided-wall column for extractive distillation. *J. Chem. Eng. Japan* 33, 627–632. <https://doi.org/10.1252/kakoronbunshu.26.627>
- Natalie, J., Czarnecki, Scott, A., Owens, Bruce Eldridge, R., 2023. Extractive Dividing Wall Column for Separating Azeotropic Systems: A Review. *Ind. Eng. Chem. Res.* 62, 5750-5770. DOI: 10.1021/acs.iecr.3c00302
- Olujić, Ž., Kaibel, B., Jansen, H., Rietfort, T., Zich, E., Frey, G., 2003. Distillation column internals/configurations for process intensification. *Chem. Biochem. Eng. Q.* 17, 301–309.
- Parkinson, G., 2007. Dividing-wall columns find greater appeal. *Chem. Eng. Prog.* 103, 8–11.
- Petlyuk, F.B., Vinogradova, E.I., Serafimov, L.A., 1984. Possible compositions of products of

- ternary azeotropic mixtures distillation at minimum reflux. *Theor. Found. Chem. Eng.* 18, 87–94.
- Petlyuk, F.B., 1998. Simple Methods for Predicting Feasible Sharp Separations of Azeotropic Mixtures. *Theor. Found. Chem. Eng.* 32, 245–253.
- Petlyuk, F.B., Danilov, R.Y., 1999a. Sharp Distillation of Azeotropic Mixtures in a Two-Feed Column. *Theor. Found. Chem. Eng.* 33, 233–242.
- Petlyuk, F.B., Danilov, R.Y., 1999b. Feasible separation variants and minimum-reflux calculations for multicomponent azeotropic mixtures. *Theor. Found. Chem. Eng.* 33, 571–583.
- Petlyuk, F.B., Danilov, R.Y., 2001a. Few-step iterative methods for distillation process design using the trajectory bundle theory: Algorithm structure. *Theor. Found. Chem. Eng.* 35, 224–236. <https://doi.org/10.1023/A:1010438123242>
- Petlyuk, F.B., Danilov, R.Y., 2001b. Theory of distillation trajectory bundles and its application to the optimal design of separation units: Distillation trajectory bundles at finite reflux. *Chem. Eng. Res. Des.* 79, 733–746. <https://doi.org/10.1205/026387601753192055>
- Petlyuk, F.B., Danilov, R.Y., 2002. Few-step iterative methods for distillation process design using trajectory bundle theory: Rigorous minimum-reflux calculation. *Theor. Found. Chem. Eng.* 36, 34–47. <https://doi.org/10.1023/A:1013945407642>
- Petlyuk, F.B., 2004. *Distillation Theory and Its Application to Optimal Design of Separation Units*. Cambridge University Press, Cambridge. <https://doi.org/10.1017/CBO9780511547102>
- Petlyuk, F.B., Danilov, R.Y., Serafimov, L.A., 2009. Feasible variants of separation in distillation of multicomponent azeotropic mixtures. *Theor. Found. Chem. Eng.* 43, 23–32. <https://doi.org/10.1134/S0040579509010047>
- Petlyuk, F.B., Danilov, R.Y., Skouras, S., Skogestad, S., 2011. Identification and analysis of possible splits for azeotropic mixtures-1. Method for column sections. *Chem. Eng. Sci.* 66, 2512–2522. <https://doi.org/10.1016/j.ces.2011.02.037>
- Petlyuk, F.B., Danilov, R.Y., Skouras, S., Skogestad, S., 2012. Identification and analysis of possible splits for azeotropic mixtures. 2. Method for simple columns. *Chem. Eng. Sci.* 69, 159–169. <https://doi.org/10.1016/j.ces.2011.10.017>
- Petlyuk, F.B., Danilov, R.Y., Burger, J., 2015. A novel method for the search and identification of

- feasible splits of extractive distillations in ternary mixtures. *Chem. Eng. Res. Des.* 99, 132–148.
<https://doi.org/10.1016/j.cherd.2015.02.013>
- Petlyuk, F.B., Danilov, R.Y., Adiche, C., 2021. Using the Method of Infinitely Sharp Splits for the Optimal Design of Extractive Distillation Units. 1. Ternary Mixtures, *Ind. Eng. Chem. Res.* 2021, 60, 16430–16444. <http://dx.doi.org/10.1021/acs.iecr.1c00715>
- Prosim, 2023. ProsimPlus steady state simulator and Simulis Thermodynamics property server. <https://www.prosim.net/en/software-in-process-simulation-optimization/>. Last accessed nov 2023.
- Rodriguez-Donis, I., Shcherbakova, N., Parascandolo, E., Abildskov, J., Gerbaud, V. 2023. Entrainer selection using the Infinitely Sharp Split method and thermodynamic criteria for separating binary minimum boiling azeotrope by extractive distillation. In preparation to be submitted to *Chem. Eng. Res. Des.*
- Rodriguez-Donis, I., Gerbaud, V., Joulia, X., 2009. Thermodynamic insights on the feasibility of homogeneous batch extractive distillation, 1. Azeotropic Mixtures with a Heavy Entrainer. *Ind. Eng. Chem. Res.* 48(7), 3544–3559. <https://doi.org/10.1021/ie801061y>
- Seihoub, F.Z., Gerbaud, V., Benyounes, H., 2022. direct and fully automated shortcut method for designing an extractive dividing wall column: 1. Minimum azeotropic Mixtures with a Heavy Entrainer. *Proceedings of the Distillation and Adsorption 2022*. (Toulouse, 18-21/10/22).
- Serafimov, L.A., 1970. The azeotropic rule and classification of multicomponents mixtures VII diagrams for ternary mixtures. *Russ. J. Phys. Chem.* 44, 567–571.
- Shen, W., Benyounes, H., Gerbaud, V., 2013. Extension of Thermodynamic Insights on Batch Extractive Distillation to Continuous Operation. 1. Azeotropic Mixtures with a Heavy Entrainer. *Ind. Eng. Chem. Res.* 52(12), 4606–4622. <https://doi.org/10.1021/ie3011148>
- Staak, D., Grützner, T., 2017. Process integration by application of an extractive dividing-wall column: An industrial case study. *Chem. Eng. Res. Des.* 123, 120–129.
<https://doi.org/10.1016/j.cherd.2017.04.003>
- Sucksmith, I., 1982. Extractive distillation saves energy. *Chem. Eng. (New York)* 89, 91–95.
- Sun, L., Wang, Q., Li, L., Zhai, J., Liu, Y., 2014. Design and control of extractive dividing wall column for separating benzene/cyclohexane mixtures. *Ind. Eng. Chem. Res.* 53, 8120–8131.

<https://doi.org/10.1021/ie500291a>

- Tavan, Y., Riazi, S.H., Nozohouri, M., 2014a. Energy optimization and comparative study of pre- and post-fractionator extractive dividing wall column for the CO₂-ethane azeotropic process. *Energy Convers. Manag.* 79, 590–598. <https://doi.org/10.1016/j.enconman.2013.12.029>
- Tavan, Y., Shahhosseini, S., Hosseini, S.H., 2014b. Design and simulation of ethane recovery process in an extractive dividing wall column. *J. Clean. Prod.* 72, 222–229. <https://doi.org/10.1016/j.jclepro.2014.03.015>
- Tututi-Avila, S., Jiménez-Gutiérrez, A., Hahn, J., 2014. Control analysis of an extractive dividing-wall column used for ethanol dehydration. *Chem. Eng. Process. Process Intensif.* 82, 88–100. <https://doi.org/10.1016/j.cep.2014.05.005>
- Waltermann, T., Grueters, T., Muenchrath, D., Skiborowski, M., 2020. Efficient optimization-based design of energy-integrated azeotropic distillation processes. *Comput. Chem. Eng.* 133, 106676. <https://doi.org/10.1016/j.compchemeng.2019.106676>
- Wang, X., Xie, L., Tian, P., Tian, G., 2016. Design and control of extractive dividing wall column and pressure-swing distillation for separating azeotropic mixture of acetonitrile/N-propanol. *Chem. Eng. Process. Process Intensif.* 110, 172–187. <https://doi.org/10.1016/j.cep.2016.10.009>
- Xia, M., Yu, B., Wang, Q., Jiao, H., Xu, C., 2012. Design and Control of Extractive Dividing-Wall Column for Separating Methylal–Methanol Mixture. *Ind. Eng. Chem. Res.* 51, 16016–16033. <https://doi.org/10.1021/ie3015395>
- Ye, Q., Wang, Y., Pan, H., Zhou, W., Peiqing, Y., 2022. Design and Control of Extractive Dividing Wall Column for Separating Dipropyl Ether/1-Propyl Alcohol Mixture. *Processes* 10, 665.
- Yildirim, Ö., Kiss, A.A., Kenig, E.Y., 2011. Dividing wall columns in chemical process industry: A review on current activities. *Sep. Purif. Technol.* 80, 403–417. <https://doi.org/10.1016/j.seppur.2011.05.009>
- Yu, J., Wang, S.J., Huang, K., Yuan, Y., Chen, H., Shi, L., 2015. Improving the Performance of Extractive Dividing-Wall Columns with Intermediate Heating. *Ind. Eng. Chem. Res.* 54, 2709–2723. <https://doi.org/10.1021/ie503148t>
- Zhang, H., Ye, Q., Qin, J., Xu, H., Li, N., 2014. Design and control of extractive dividing-wall

- column for separating ethyl acetate-isopropyl alcohol mixture. *Ind. Eng. Chem. Res.* 53, 1189–1205. <https://doi.org/10.1021/ie403618f>
- Zhang, Z., Wang, C., Guang, C., Wang, C., 2019. Separation of propylene oxide-methanol-water mixture via enhanced extractive distillation: Design and control. *Chem. Eng. Process. - Process Intensif.* 144, 107651. <https://doi.org/10.1016/j.cep.2019.107651>
- Zhang, Z., Zhao, X., Zhu, X., Li, M., Ma, Z., Gao, J., 2021. Energy-saving exploration and optimization of methyl alcohol – Methyl ethyl ketone – Tertbutyl alcohol separation by extractive dividing-wall distillation with ionic liquid as extractant. *Sep. Purif. Technol.* 272, 118886. <https://doi.org/10.1016/j.seppur.2021.118886>
- Zhu, J., Jing, C., Hao, L., Wei, H., 2021. Insight into controllability and operation of extractive dividing-wall column. *Sep. Purif. Technol.* 263, 118362. <https://doi.org/10.1016/j.seppur.2021.118362>
- Wu, Y., Hsu, P.H.C., Chien, L.L., 2013. Critical assesment of the energy saving potential of an extractive dividing wall column. *Ind. Eng. Chem.Res.* 52(15), 5384-5399. <https://doi.org/10.1021/ie3035898>